arXiv:2212.06319v2 [math.OC] 14 Jan 2023

Linear Convergence of ISTA and FISTA*

Bowen Li Bin Shi† Ya-xiang Yuan

State Key Laboratory of Scientific and Engineering Computing, Academy of Mathematics and Systems Science, Chinese Academy of Sciences, Beijing 100190, China
University of Chinese Academy of Sciences, Beijing 100049, China

January 18, 2023

Abstract

In this paper, we revisit the class of iterative shrinkage-thresholding algorithms (ISTA) for solving the linear inverse problem with sparse representation, which arises in signal and image processing. It is shown in the numerical experiment to deblur an image that the convergence behavior in the logarithmic-scale ordinate tends to be linear instead of logarithmic, approximating to be flat. Making meticulous observations, we find that the previous assumption for the smooth part to be convex weakens the least-square model. Specifically, assuming the smooth part to be strongly convex is more reasonable for the least-square model, even though the image matrix is probably ill-conditioned. Furthermore, we improve the pivotal inequality tighter for composite optimization with the smooth part to be strongly convex instead of general convex, which is first found in [Li et al., 2022]. Based on this pivotal inequality, we generalize the linear convergence to composite optimization in both the objective value and the squared proximal subgradient norm. Meanwhile, we set a simple ill-conditioned matrix which is easy to compute the singular values instead of the original blur matrix. The new numerical experiment shows the proximal generalization of Nesterov's accelerated gradient descent (`NAG`) for the strongly convex function has a faster linear convergence rate than ISTA. Based on the tighter pivotal inequality, we also generalize the faster linear convergence rate to composite optimization, in both the objective value and the squared proximal subgradient norm, by taking advantage of the well-constructed Lyapunov function with a slight modification and the phase-space representation based on the high-resolution differential equation framework from the implicit-velocity scheme.

1 Introduction

In scientific and engineering computation, the class of so-called inverse problems is to infer and calculate the causes according to the observations or effects, which is just the reverse of the forward inference from the causes to the effects. Specifically, the inverse problems involve determining the parameters of a system that cannot be observed directly. Since the eighties of the last century, it has become the fastest growing field, regardless of theory or algorithm, due to its wide range of applications, such as signal and image processing, statistical inference, geophysics, astrophysics, and so on [Engl et al., 1996].

*This work was supported by Grant No.YSBR-034 of CAS and Grant No.12288201 of NSFC.
†Corresponding author, Email: `shibin@lsec.cc.ac.cn`

Perhaps the simplest and classical one is the class of linear inverse problems, e.g., the image deblurring problem. Recall we deblur the image of an elephant with the pixel 256×256 in [Li et al., 2022], which is implemented by the class of iterative shrinkage-thresholding algorithms (ISTA) as

$$y_{k+1} = y_k - sG_s(y_k),$$

with any initial $y_0 = x_0 \in \mathbb{R}^d$ and a fixed step size $s \in (0, 1/L]$, where $G_s(\cdot)$ is the s-proximal subgradient operator.[1] We show the convergence behavior of the squared s-proximal subgradient norm in Figure 1, where the regularization parameter is set as $\lambda = 10^{-6}$ and the step size $s = 0.5$. Based on the assumption of the convex function, we derive that the minimal squared s-proximal subgradient norm obeys the sublinear convergence, concretely $o(1/k^3)$, in [Li et al., 2022]. However, with a black dashed line as a comparison, we find the convergence rate of the squared s-proximal subgradient norm tends to be linear instead of logarithmic $\sim -3 \log k$, approximating to be flat. In other words, the objective function is more like the μ-strongly convex function rather than the convex function.

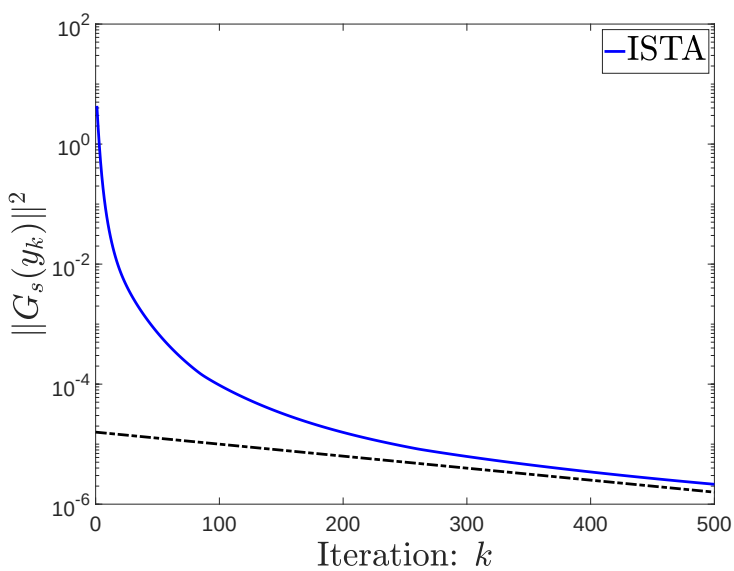

Figure 1: The convergence behavior of the squared s-proximal subgradient norm by implementing ISTA to deblur the image of an elephant, shown in [Li et al., 2022, Figure 1 & Figure 2].

Numerical Phenomena Recall the linear inverse problem with sparse representation is formulated by the least square (or linear regression) model with ℓ_1-regularization in [Beck and Teboulle, 2009] as

$$\frac{1}{2}\|Ax - b\|^2 + \lambda\|x\|_1, \tag{1.1}$$

[1] The Lipschitz constant L and the s-proximal subgradient operator $G_s(\cdot)$ are defined rigorously in Definition 2.5 and Definition 2.6, respectively.

where $A \in \mathbb{R}^{m\times d}$ is an $m \times d$ matrix, $b \in \mathbb{R}^m$ is an m-dimensional vector, and the regularization parameter $\lambda > 0$ is a tradeoff between fidelity to the measurements and noise sensitivity.[2] Here for the least square model with ℓ_1-regularization (1.1), we note $\lambda_i(A^TA)$, $(i = 1, \ldots, d)$ as the eigenvalues for the symmetric matrix A^TA. Then, the parameters used for the optimization satisfy $\mu = \min_{1\le i\le d} \lambda_i(A^TA)$ and $L = \max_{1\le i\le d} \lambda_i(A^TA)$, respectively. In addition, the condition number is noted as

$$\mathbf{cond}(A^TA) = \frac{L}{\mu} = \frac{\max\limits_{1\le i\le d} \lambda_i(A^TA)}{\min\limits_{1\le i\le d} \lambda_i(A^TA)}.$$

Practically, the matrix A in the least square model with ℓ_1-regularization (1.1) is ill-conditioned for the linear inverse problems [Hansen et al., 2006, Figueiredo et al., 2007], that is, the condition number $\mathbf{cond}(A^TA)$ is very large.

To further observe the phenomenon of the linear convergence discovered in Figure 1, we conduct a new numerical experiment by setting the ill-conditioned matrix A and the vector b manually. Concretely, we set A as a 500×500 tridiagonal matrix with $A_{i,i} = 2,\ A_{i,i+1} = 1,\ A_{i+1,i} = 1$ and b as a 500-dimensional vector with every entry $b_i = 1$. Taking some simple computations, we obtain the optimization parameters as $\mu = \min_{1\le i\le d} \lambda_i(A^TA) = 1.5461 \times 10^{-9}$ and $L = \max_{1\le i\le d} \lambda_i(A^TA) = 15.9997$, respectively. Obviously, the matrix A is ill-conditioned since the condition number is $\mathbf{cond}(A^TA) \approx 1 \times 10^{-10}$. Meanwhile, this also manifests that setting the step size $s = 0.05 < 1/L$ is reasonable. Finally, we show the numerical experiment by implementing ISTA with the same regularization parameter $\lambda = 10^{-6}$ in Figure 2, where the linear convergence behavior of the squared proximal subgradient norm is more predominant after several iterations.

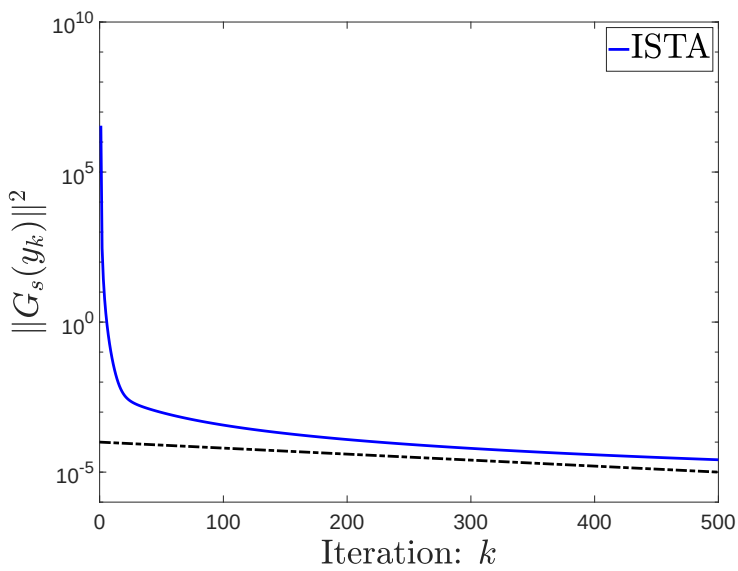

Figure 2: The convergence behavior of the squared s-proximal subgradient norm by implementing ISTA in the least square model with ℓ_1-regularization.

[2]Throught the paper, $\|\cdot\|$ denotes the standard Euclidean norm without any special emphasization and labeling. And $\|\cdot\|_1$ denotes the ℓ_1-norm as $\|x\|_1 = \sum_{i=1}^d |x_i|$ for any $x \in \mathbb{R}^d$.

For the smooth case, Nesterov's accelerated gradient descent (NAG) globally accelerates the convergence rate of the vanilla gradient descent for the μ-strongly convex function. Naturally, we hope to investigate the proximal version of NAG as

$$\begin{cases} x_k = y_{k-1} - sG_s(y_{k-1}), \\ y_k = x_k + \dfrac{x_k - x_{k-1}}{1 + 2\sqrt{\mu s}}, \end{cases}$$

with any initial $x_0 = y_0 \in \mathbb{R}^d$, which is also called the class of fast iterative shrinkage-thresholding algorithms, shortened as FISTA.[3] Thus, a new numerical experiment by adding FISTA for comparison is show in Figure 3. Similarly, we also add a black dashed line as a basis to characterize the worst convergence rate of the squared s-proximal gradient norm by implementing FISTA. By comparing the two dashed lines in Figure 3, we find that the acceleration phenomenon indeed exists for the squared s-proximal subgradient norm of FISTA beyond ISTA.

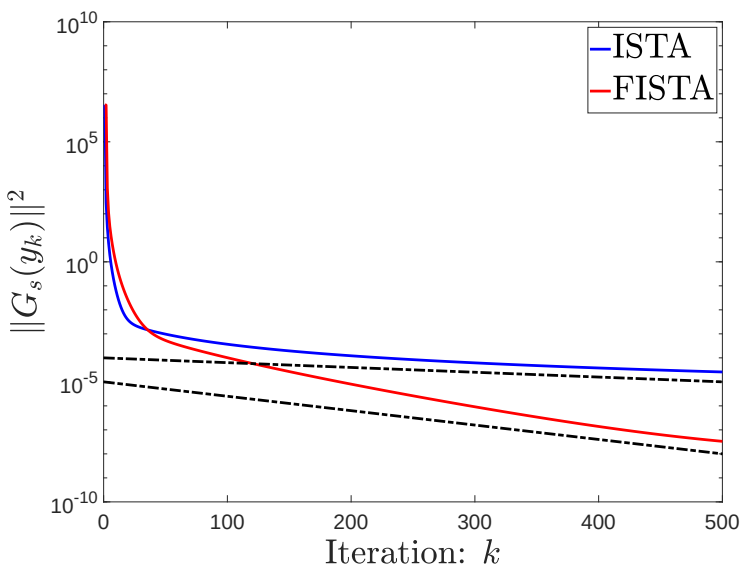

Figure 3: The convergence behavior of the squared proximal subgradient norm by implementing ISTA and FISTA in the least square model with ℓ_1-regularization.

1.1 Main contributions

From the description above, the linear inverse problem with sparse representation is formulated as the least-square model with ℓ_1-regularization (1.1). In the language of optimization, it corresponds to composite optimization

$$\min_{x \in \mathbb{R}^d} \Phi(x) := f(x) + g(x), \tag{1.2}$$

[3]The FISTA here is a proximal generalization of NAG for the μ-strongly convex function, and different from that in [Beck and Teboulle, 2009], which is based on NAG for the convex function. In addition, the momentum coefficient here has a little modification, which is first proposed in [Chen et al., 2022b] to provide a tailor-made proof.

where f is a μ-strongly smooth convex function and g is a continuous convex function that is possibly not smooth. For the composite optimization problem (1.2), we make the following contributions.

The pivotal inequality for composite optimization From the smooth case, the pivotal inequality for the convex function is observed in [Li et al., 2022] as

$$f(y - s\nabla f(y)) - f(x) \leq \langle \nabla f(y), y - x\rangle - \left(s - \frac{s^2 L}{2}\right) \|\nabla f(y)\|^2. \tag{1.3}$$

And then, we generalize (1.3) to composite optimization to derive the s-proximal subgradient norm minimization of ISTA and FISTA. Similarly, it is observed here that the pivotal inequality (1.3) can be improved tighter to the μ-strongly convex function as

$$f(y - s\nabla f(y)) - f(x) \leq \langle \nabla f(y), y - x\rangle - \frac{\mu}{2}\|y - x\|^2 - \left(s - \frac{s^2 L}{2}\right) \|\nabla f(y)\|^2. \tag{1.4}$$

We generalize the pivotal inequality (1.4) to the composite objective function in Section 3.

Linear convergence of ISTA Recall the squared distance as the Lyapunov function in [Shi et al., 2019, Theorem A.4] is used to derive the linear convergence.[4] Based on the proximal version of the pivotal inequality (1.4), we obtain the convergence rate of ISTA for both the objective value and the s-proximal subgradient norm square, respectively as

$$\Phi(y_k) - \Phi(x^\star) \leq O\left(\left(\frac{1-\mu s}{1+\mu s}\right)^k\right) \quad \text{and} \quad \|G_s(y_k)\|^2 \leq O\left(\left(\frac{1-\mu s}{1+\mu s}\right)^k\right)$$

for any $0 < s \leq 1/L$. Moreover, the s-proximal subgradient norm is convenient to be used in practice, where the minimization rate is consistent with the numerical phenomena in Figure 1 and Figure 2.

Accelerated linear convergence of FISTA Recall the Lyapunov function constructed from the implicit-velocity in [Chen et al., 2022b] is used to obtain the linear convergence. Here, we take a modification for the potential energy using x_k instead of y_k. Combined with the proximal version of the pivotal inequality (1.4), we obtain the convergence rate of FISTA, respectively as:

(1) For the objective value, it follows

$$\Phi(x_k) - \Phi(x^\star) \leq O\left(\frac{1}{\left(1 + \frac{\sqrt{\mu s}}{4}\right)^k}\right)$$

with any step size $0 < s \leq 1/L$;

[4] It should be noted that Nesterov [1998, Theorem 2.1.15] use the squared norm to derive the convergence rate, which is only recounted by the language of the Lyapunov function in [Shi et al., 2019, Theorem A.4].

(2) for the squared s-proximal subgradient norm, it follows

$$\|G_s(y_k)\|^2 \leq O\left(\frac{1}{\left(1+\frac{\sqrt{\mu s}}{4}\right)^k}\right)$$

with any step size $0 < s < 1/L$.

Similarly, the minimization rate of the squared s-proximal subgradient norm is consistent with the numerical phenomenon observed in Figure 3.

1.2 Related works and organization

Recall the history of first-order smooth optimization, Nesterov [1983] proposed `NAG` for the convex function and the "*Estimate Sequence*" technique to bring about the global acceleration phenomenon, which was also generalized to the μ-strongly convex function in [Nesterov, 1998]. Furthermore, [Nesterov, 2010] points out that the algorithmic structures are very close in both `NAG` for the μ-strongly convex function and Polyak's heavy-ball method [Polyak, 1964]. And then, this view is emphasized further in [Jordan, 2018]. Finally, the veil behind the acceleration phenomenon is lifted by the discovery of gradient correction based on the high-resolution differential equation framework in [Shi et al., 2022]. Recently, the high-resolution differential equation framework from the implicit-velocity scheme is found to be perfect and superior to the gradient-correction scheme in [Chen et al., 2022b].

The technique of Lyapunov analysis used to investigate the acceleration phenomenon dates from [Su et al., 2016] for the convex function. Besides capturing the acceleration mechanism, the Lyapunov function based on this high-resolution differential framework leads to the gradient norm minimization in [Shi et al., 2022]. The tailor-made proofs and the equivalent implicit-velocity effect are shown in [Chen et al., 2022a]. With the observation to the key inequality, the gradient norm minimization is generalized to the composite function in [Li et al., 2022]. It is proposed by combining the low-resolution differential equation and the continuous limit of the Newton method to design and analyze new algorithms in [Attouch et al., 2020], where the terminology is called inertial dynamics with a Hessian-driven term. Although the inertial dynamics with a Hessian-driven term resembles closely with the high-resolution differential equations in [Shi et al., 2022], it is important to note that the Hessian-driven terms are from the second-order information of Newton's method [Attouch et al., 2014], while the gradient correction entirely relies on the first-order information of Nesterov's accelerated gradient descent method itself.

The remainder of this paper is organized as follows. In Section 2, we collect some basic definitions and theorems as preliminaries. We provide two key inequalities for composite functions with rigorous proofs in Section 3. The convergence rate of ISTA for both the objective value and the s-proximal subgradient norm square is shown in Section 4. And we demonstrate the convergence rate of FISTA for both the objective value and the s-proximal subgradient norm square from the implicit-velocity scheme in Section 5. In Section 6, we propose a conclusion and discuss some further research works.

2 Preliminaries

In this section, we collect some basic definitions and theorems from the classical books [Nesterov, 1998] and [Rockafellar, 1970] with slight modifications for later uses in the following sections. First, some basic definitions in convex optimization are described from [Nesterov, 1998], e.g., convex functions, subgradients, and subdifferentials.

Definition 2.1. *A continuous function $g = g(x)$ defined on $\mathbb{R}^d$ is convex if for any $\alpha \in [0, 1]$, the following inequlaity holds*

$$g(\alpha x + (1-\alpha)y) \leq \alpha g(x) + (1-\alpha)g(y)$$

for any $x, y \in \mathbb{R}^d$. Moreover, we note $\mathcal{F}^0(\mathbb{R}^d)$ as the class of continuous convex functions.

Definition 2.2. *Let $g \in \mathcal{F}^0(\mathbb{R}^d)$. A vector v is called a subgradient of g at x if for any $y \in \mathbb{R}^d$, we have*

$$g(y) \geq g(x) + \langle v, y - x \rangle.$$

Moreover, the set of all subgradients of $g \in \mathcal{F}^0(\mathbb{R}^d)$ at x is called the subdifferential of g at x, and we note it as $\partial g(x)$.

Then, we collect two theorems from [Rockafellar, 1970] to characterize the basic properties of subdifferentials and subgradients.

Theorem 2.3 (Theorem 23.8 in [Rockafellar, 1970])**.** *Let $g_1, g_2 \in \mathcal{F}^0(\mathbb{R}^d)$. Then the subdifferentials satisfy*

$$\partial(g_1 + g_2)(x) = \partial g_1(x) + \partial g_2(x)$$

for any $x \in \mathbb{R}^d$.

Theorem 2.4 (Theorem 25.1 in [Rockafellar, 1970])**.** *Let $g \in \mathcal{F}^0(\mathbb{R}^d)$. If g is differentiable at x, then $\nabla g(x)$ is the unique subgradient of g at x, so that in particular*

$$g(y) \geq g(x) + \langle \nabla g(x), y - x \rangle,$$

for any $y \in \mathbb{R}^d$.

Next, we define the μ-strongly convex function instead of the general convex function for the smooth part in the composite function to characterize the least-square model.

Definition 2.5. *Let $f \in \mathcal{F}^0(\mathbb{R}^d)$. The function f is L-smooth if f is differentiable and the gradient of f satisfies*

$$\|\nabla f(x) - \nabla f(y)\| \leq L\|x - y\|$$

for any $x, y \in \mathbb{R}^d$. The function f is μ-strongly convex if f is differentiable and satisfies

$$f(y) \geq f(x) + \langle \nabla f(y), y - x \rangle + \frac{\mu}{2}\|y - x\|^2$$

for any $x, y \in \mathbb{R}^d$. The subclass of $\mathcal{F}^0(\mathbb{R}^d)$ with the L-smoothness and μ-strongly convexity is noted as $\mathcal{S}^1_{\mu,L}(\mathbb{R}^d)$.

In this paper, we consider the composite function $\Phi = f + g$ with $f \in \mathcal{S}^1_{\mu,L}$ and $g \in \mathcal{F}^0$ and note $x^\star$ as its unique minimizer. Finally, we provide the definitions of both the s-proximal operator and the s-proximal subgradient operator originally shown in [Beck and Teboulle, 2009, Su et al., 2016] as

Definition 2.6. *For any $f \in \mathcal{S}^1_{\mu,L}$ and $g \in \mathcal{F}^0$, the s-proximal operator is defined as*

$$P_s(x) := \arg\min_{y \in \mathbb{R}^d} \left\{ \frac{1}{2s} \|y - (x - s\nabla f(x))\|^2 + g(y) \right\}, \tag{2.1}$$

for any $x \in \mathbb{R}^d$. Furthermore, the s-proximal subgradient operator is defined as

$$G_s(x) := \frac{x - P_s(x)}{s} \tag{2.2}$$

for any $x \in \mathbb{R}^d$.

When g is reduced to the ℓ_1-norm, that is, $g(x) = \lambda\|x\|_1$, we can derive the closed-form expression of the s-proximal operator (2.1) at any $x \in \mathbb{R}^d$ for the special case as

$$P_s(x)_i = \big(|(x - s\nabla f(x))_i| - \lambda s \big)_+ \mathrm{sgn}\big((x - s\nabla f(x))_i \big),$$

where $i = 1, \ldots, d$ is the index.

3 Two inequalities for composite optimization

In this section, based on the basic definitions and theorems shown in Section 2, we generalize two basic inequalities of $f \in \mathcal{S}^1_{\mu,L}$ to the composite function $\Phi = f + g$ with $f \in \mathcal{S}^1_{\mu,L}$ and $g \in \mathcal{F}^0$.

Lemma 3.1. *Let $f \in \mathcal{S}^1_{\mu,L}(\mathbb{R}^d)$ and $g \in \mathcal{F}^0(\mathbb{R}^d)$. Then the composite function $\Phi = f + g$ satisfies*

$$\Phi(x) - \Phi(x^\star) \geq \frac{\mu}{2}\|x - x^\star\|^2 \tag{3.1}$$

Proof of Lemma 3.1. With Definition 2.1 and Definition 2.2, the basic convex inequality holds for any subgradient $v \in \partial\Phi(x^\star)$ as

$$\Phi(x) \geq \Phi(x^\star) + \langle v, x - x^\star \rangle$$

with any $x \in \mathbb{R}^d$. Since $x^\star$ is the unique global minimizer, we know that zero is a subgradient, that is, $0 \in \partial\Phi(x^\star)$. Meanwhile, due to $f \in \mathcal{S}^1_{\mu,L}(\mathbb{R}^d)$, we obtain the basic inequality for the μ-strongly convex function as

$$f(x) \geq f(x^\star) + \langle \nabla f(x^\star), x - x^\star \rangle + \frac{\mu}{2}\|x - x^\star\|^2 \tag{3.2}$$

with any $x \in \mathbb{R}^d$; and since $g \in \mathcal{F}^0(\mathbb{R}^d)$, the basic convex inequality holds for any subgradient $v' \in \partial g(x^\star)$ as

$$g(x) \geq g(x^\star) + \langle v', x - x^\star \rangle \tag{3.3}$$

with any $x \in \mathbb{R}^d$. Combined with (3.2) and (3.3), we have

$$\Phi(x) \geq \Phi(x^\star) + \langle \nabla f(x^\star) + v', x - x^\star \rangle + \frac{\mu}{2}\|x - x^\star\|^2 \tag{3.4}$$

with any $x \in \mathbb{R}^d$. Furthermore, with Theorem 2.3 and Theorem 2.4, we obtain that for any $v \in \partial\Phi(x^\star)$, there exists a subgradient $v' \in \partial g(x^\star)$ such that $v = \nabla f(x^\star) + v'$. With $0 \in \partial\Phi(x^\star)$, we complete the proof. □

Recall the proof of the pivotal inequality for composite optimization [Li et al., 2022, Lemma 3.1]. Nevertheless, the function class here is $\mathcal{S}^1_{\mu,L}$ instead of $\mathcal{F}^1_L$, we can make the basic convex inequality in [Li et al., 2022, (3.5a)] tighter as

$$f(x) \geq f(y) + \langle \nabla f(y), x - y \rangle + \frac{\mu}{2}\|x - y\|^2$$

for any $x, y \in \mathbb{R}^d$, which brings about the pivotal inequality [Li et al., 2022, (3.1)] to be tighter. Hence, we provide a rigorous description to conclude this section in the following theorem.

Lemma 3.2. *Let $\Phi = f + g$ be a composite function with $f \in \mathcal{S}^1_{\mu,L}(\mathbb{R}^d)$ and $g \in \mathcal{F}^0(\mathbb{R}^d)$. Then, the following inequality*

$$\Phi(y - G_s(y)) \leq \Phi(x) + \langle G_s(y), y - x \rangle - \left(s - \frac{s^2 L}{2}\right)\|G_s(y)\|^2 - \frac{\mu}{2}\|y - x\|^2 \tag{3.5}$$

holds for any $x, y \in \mathbb{R}^d$.

4 Linear convergence of ISTA

In this section, we investigate the convergence rate of ISTA for composite optimization in both the objective value and the squared s-proximal subgradient norm. Similar to the smooth case in [Shi et al., 2019, Theorem A.4], we construct the Lyapunov function for the composite function as the squared distance, i.e.,

$$\mathcal{E}(k) = \|y_k - x^\star\|^2.^{5} \tag{4.1}$$

With the discrete Lyapunov function (4.1), we show the convergence rate in the following theorem.

Theorem 4.1. *Let $\Phi = f + g$ be a composite function with $f \in \mathcal{S}^1_{\mu,L}(\mathbb{R}^d)$ and $g \in \mathcal{F}^0(\mathbb{R}^d)$. Taking any step size $0 < s \leq 1/L$, the iterative sequence $\{y_k\}_{k=0}^\infty$ generated by ISTA satisfies*

$$\begin{cases} \Phi(y_k) - \Phi(x^\star) \leq \dfrac{1}{s}\left(\dfrac{1 - \mu s}{1 + \mu s}\right)^k \|x_0 - x^\star\|^2, & \text{(4.2a)} \\ \|G_s(y_k)\|^2 \leq \dfrac{4}{s^2}\left(\dfrac{1 - \mu s}{1 + \mu s}\right)^k \|x_0 - x^\star\|^2. & \text{(4.2b)} \end{cases}$$

Proof of Theorem 4.1. Putting the sequence $\{y_k\}_{k=0}^\infty$ generated by ISTA and the unique minimizer $x^\star$ into (3.5), Lemma 3.1 brings about the following inequality as

$$\Phi(y_{k+1}) - \Phi(x^\star) \leq \langle G_s(y_k), y_k - x^\star \rangle - \frac{s}{2}\|G_s(y_k)\|^2 - \frac{\mu}{2}\|y_k - x^\star\|^2. \tag{4.3}$$

Furthermore, with the pivotal inequality (4.3), we derive that the objective value satisfies the following inequality as

$$\Phi(y_{k+1}) - \Phi(x^\star) \leq \frac{\|y_k - x^\star\|^2}{2s} - \frac{\|y_k - x^\star - sG_s(y_k)\|^2}{2s}; \tag{4.4}$$

[5] It should be noted that Nesterov [1998, Theorem 2.1.15] use the squared norm to derive the convergence rate, which is only recounted by the language of the Lyapunov function in [Shi et al., 2019, Theorem A.4].

and with the Cauchy-Schwarz inequality, the squared s-proximal subgradient norm satisfies the following inequality as

$$\|G_s(y_k)\|^2 \leq \frac{4\|y_k - x^\star\|^2}{s^2}. \tag{4.5}$$

Then, we calculate the iterative difference of the Lyapunov function as

$$\begin{aligned}
\mathcal{E}(k+1) - \mathcal{E}(k) &= \|y_{k+1} - x^\star\|^2 - \|y_k - x^\star\|^2 \\
&= \|y_k - sG_s(y_k) - x^\star\|^2 - \|y_k - x^\star\|^2 \\
&= -2s\langle G_s(y_k), y_k - x^\star\rangle + s^2\|G_s(y_k)\|^2 \\
&\leq -2s\left(\Phi(y_{k+1}) - \Phi(x^\star)\right) - s\mu\|y_k - x^\star\|^2
\end{aligned}$$

where the last inequality follows from (4.3). With Lemma 3.1, we can obtain further

$$\|y_{k+1} - x^\star\|^2 \leq (1 - s\mu)\|y_k - x^\star\|^2 - \mu s\|y_{k+1} - x^\star\|^2,$$

which directly leads to the linear convergence of the Lyapunov function as

$$\mathcal{E}(k) = \|y_k - x^\star\|^2 \leq \left(\frac{1 - \mu s}{1 + \mu s}\right)\|x_0 - x^\star\|^2. \tag{4.6}$$

From (4.4), (4.5) and (4.6), we derive the linear rates in (4.2a) and (4.2b), conseqently the proof is complete. □

We conclude this section with the following corollary by setting the step size $s = 1/L$.

Corollary 4.2. *When the step size is set $s = 1/L$, the iterative sequence $\{y_k\}_{k=0}^\infty$ generated by ISTA satisfies*

$$\Phi(y_k) - \Phi(x^\star) \leq L\left(\frac{L - \mu}{L + \mu}\right)^k \|x_0 - x^\star\|^2, \tag{4.7}$$

$$\|G_s(y_k)\|^2 \leq 4L^2\left(\frac{L - \mu}{L + \mu}\right)^k \|x_0 - x^\star\|^2. \tag{4.8}$$

5 Accelerated linear convergence of FISTA

In this section, we investigate the convergence rate of FISTA for composite optimization in both the objective value and the squared s-proximal subgradient norm. Here, we choose the phase-space representation of FISTA from the implicit-velocity scheme as

$$\begin{cases} x_{k+1} - x_k = \sqrt{s}v_{k+1}, \\ v_{k+1} - v_k = -\dfrac{2\sqrt{\mu s}v_k}{1 + 2\sqrt{\mu s}} - \sqrt{s}G_s(y_k), \end{cases} \tag{5.1}$$

with any initial $x_0 \in \mathbb{R}^d$ and $v_0 = 0$, where the iterative sequence $\{y_k\}_{k=0}^\infty$ satisfies

$$y_k = x_k + \frac{\sqrt{s}v_k}{1 + 2\sqrt{\mu s}}. \tag{5.2}$$

Similar to [Chen et al., 2022a], we move one space backward for the discrete Lyapunov function constructed in [Chen et al., 2022b] as

$$\mathcal{E}(k) = \underbrace{\Phi(x_k) - \Phi(x^\star)}_{\mathcal{E}_{\mathbf{pot}}(k)} + \underbrace{\frac{\|v_k\|^2}{4(1+2\sqrt{\mu s})^2}}_{\mathcal{E}_{\mathbf{kin}}(k)} + \underbrace{\frac{\left\|v_k + 2\sqrt{\mu}(x_k - x^\star)\right\|^2}{4}}_{\mathcal{E}_{\mathbf{mix}}(k)}. \tag{5.3}$$

In (5.3), we use the iterative sequence $\{x_k\}_{k=0}^\infty$ instead of $\{y_k\}_{k=0}^\infty$ for the potential energy, which is because the proof for composite optimization is essentially dependent on the pivotal inequality (3.5). The convergence rate is formulated rigorously in the following theorem.

Theorem 5.1. *Let $\Phi = f + g$ be a composite function with $f \in \mathcal{S}^1_{\mu,L}(\mathbb{R}^d)$ and $g \in \mathcal{F}^0(\mathbb{R}^d)$. Taking any step size $0 < s \le 1/L$, the iterative sequence $\{x_k\}_{k=0}^\infty$ generated by FISTA satisfies*

$$\Phi(x_k) - \Phi(x^\star) \le \frac{\Phi(x_0) - \Phi(x^\star) + \mu\|x_0 - x^\star\|^2}{\left(1 + \frac{\sqrt{\mu s}}{4}\right)^k}; \tag{5.4}$$

if the step size satisfies $0 < s < 1/L$, the iterative sequence $\{y_k\}_{k=0}^\infty$ satisfies

$$\|G_s(y_k)\|^2 \le \frac{2\left(\Phi(x_0) - \Phi(x^\star) + \mu\|x_0 - x^\star\|^2\right)}{s(1-sL)\left(1 + \frac{\sqrt{\mu s}}{4}\right)^k}. \tag{5.5}$$

Proof of Theorem 5.1. First, we present the calculation of the Lyapunov function's iterative difference in three steps, similarly with [Chen et al., 2022b].

(1) First, we start from the mixed energy $\mathcal{E}_{\mathbf{mix}}(k)$. The critical point to calculating the iterative difference lies in

$$[v_{k+1} + 2\sqrt{\mu}(x_{k+1} - x^\star)] - [v_k + 2\sqrt{\mu}(x_k - x^\star)] = -\sqrt{s}G_s(y_k),$$

which directly follows the implicit-velocity phase-space representation (5.1) and (5.2). Then, we calculate the iterative difference of the mixed energy as

$$\begin{aligned}
\mathcal{E}_{\mathbf{mix}}(k+1) - \mathcal{E}_{\mathbf{mix}}(k) =& \frac{1}{4}\left\|v_{k+1} + 2\sqrt{\mu}(x_{k+1} - x^\star)\right\|^2 - \frac{1}{4}\left\|v_k + 2\sqrt{\mu}(x_k - x^\star)\right\|^2 \\
=& \frac{1}{2}\left\langle -\sqrt{s}G_s(y_k), v_k + 2\sqrt{\mu}(x_k - x^\star)\right\rangle + \frac{s}{4}\|G_s(y_k)\|^2 \\
=& \frac{1}{2}\left\langle -\sqrt{s}G_s(y_k), \frac{v_k}{1+2\sqrt{\mu s}} + 2\sqrt{\mu}(y_k - x^\star)\right\rangle + \frac{s}{4}\|G(y_k)\|^2,
\end{aligned}$$

where the last inequality also follows from (5.2). Furthermore, with the second scheme of (5.1), we obtain the iterative difference as

$$\mathcal{E}_{\mathbf{mix}}(k+1) - \mathcal{E}_{\mathbf{mix}}(k) = -\frac{\sqrt{s}}{2}\left\langle G_s(y_k), v_{k+1}\right\rangle - \sqrt{\mu s}\left\langle G_s(y_k), y_k - x^\star\right\rangle - \frac{s}{4}\|G_s(y_k)\|^2. \tag{5.6}$$

(2) Then, we consider the kinetic energy $\mathcal{E}_{\mathbf{kin}}(k)$. The detailed calculation of iterative difference is shown as

$$\begin{aligned}\mathcal{E}_{\mathbf{kin}}(k+1)-\mathcal{E}_{\mathbf{kin}}(k) &= \frac{\|v_{k+1}\|^2}{4(1+2\sqrt{\mu s})^2}-\frac{\|v_k\|^2}{4(1+2\sqrt{\mu s})^2}\\ &= \frac{\|v_{k+1}\|^2}{4(1+2\sqrt{\mu s})^2}-\frac{\|v_{k+1}+\sqrt{s}G_s(y_k)\|^2}{4}\\ &= -\frac{\sqrt{s}}{2}\langle G_s(y_k),v_{k+1}\rangle-\frac{\sqrt{\mu s}\|v_{k+1}\|^2}{(1+2\sqrt{\mu s})^2}-\frac{s}{4}\|G_s(y_k)\|^2, \end{aligned} \tag{5.7}$$

where the second equality follows from the second scheme of (5.1).

(3) In the last step, we turn to the potential energy $\mathcal{E}_{\mathbf{pot}}(k)$. Recall in [Chen et al., 2022b, Section 4.2], the calculation of iterative difference is based on the basic L-smooth inequality. Here for the composite optimization, we plug x_k and x_{k+1} generated by FISTA into (3.5) to derive the inequality as

$$\Phi(x_{k+1})-\Phi(x_k)\le\langle G_s(y_k),y_k-x_k\rangle-\left(s-\frac{s^2L}{2}\right)\|G_s(y_k)\|^2, \tag{5.8}$$

which is the essential difference from the smooth case. Then with (5.8), we calculate the iterative difference as

$$\begin{aligned}\mathcal{E}_{\mathbf{pot}}(k+1)-\mathcal{E}_{\mathbf{pot}}(k) &= \Phi(x_{k+1})-\Phi(x_k)\\ &\le \langle G_s(y_k),y_k-x_k\rangle-\left(s-\frac{s^2L}{2}\right)\|G_s(y_k)\|^2\\ &= \langle G_s(y_k),x_{k+1}-x_k\rangle+s\|G_s(y_k)\|^2-\left(s-\frac{s^2L}{2}\right)\|G_s(y_k)\|^2\\ &= \sqrt{s}\langle G_s(y_k),v_{k+1}\rangle+\frac{s}{2}\|G_s(y_k)\|^2-\frac{s(1-sL)}{2}\|G_s(y_k)\|^2, \end{aligned} \tag{5.9}$$

where the second equality follows from the gradient step of FISTA.

Using the three iterative differences (5.6), (5.7) and (5.9), we obtain the iterative difference of the Lyapunov function as

$$\mathcal{E}(k+1)-\mathcal{E}(k)\le-\sqrt{\mu s}\,\langle G_s(y_k),y_k-x^\star\rangle-\frac{(\sqrt{\mu s}+\mu s)\|v_{k+1}\|^2}{(1+2\sqrt{\mu s})^2}-\frac{s(1-sL)}{2}\|G_s(y_k)\|^2. \tag{5.10}$$

Putting the sequence x_{k+1} generated by FISTA and the unique minimizer $x^\star$ into (3.5), we can see that Lemma 3.1 brings about the following inequality as

$$\Phi(x_{k+1})-\Phi(x^\star)\le\langle G_s(y_k),y_k-x^\star\rangle-\left(s-\frac{sL^2}{2}\right)\|G_s(y_k)\|^2-\frac{\mu}{2}\|y_k-x^\star\|^2. \tag{5.11}$$

It follows from (5.11) and (5.10) that

$$\mathcal{E}(k+1)-\mathcal{E}(k)$$

$$\leq -\sqrt{\mu s}\left[\Phi(x_{k+1})-\Phi(x^\star)+\frac{(1+\sqrt{\mu s})\|v_{k+1}\|^2}{(1+2\sqrt{\mu s})^2}+\frac{\mu\|y_k-x^\star\|^2}{2}\right]-\frac{s(1-sL)}{2}\|G_s(y_k)\|^2. \quad (5.12)$$

With the gradient step of FISTA, we estimate the mixed energy by Cauchy-Schwarz inequality as

$$\begin{aligned}\|v_{k+1}+2\sqrt{\mu}(x_{k+1}-x^\star)\|^2 &= \|v_{k+1}+2\sqrt{\mu}(y_k-sG_s(y_k)-x^\star)\|^2\\ &\leq 2\|v_{k+1}\|^2+8\mu\|y_k-sG_s(y_k)-x^\star\|^2\\ &= 2\|v_{k+1}\|^2+8\mu\|y_k-x^\star\|^2+8\mu s^2\|G_s(y_k)\|^2-16\mu s\langle G_s(y_k),y_k-x^\star\rangle\\ &\leq 2\|v_{k+1}\|^2+8\mu\|y_k-x^\star\|^2,\end{aligned}$$

where the last inequality follows (5.11) and (3.1). Furthermore, we estimate the discrete Lyapunov function (5.3) as

$$\mathcal{E}(k)\leq \Phi(x_k)-\Phi(x^\star)+\frac{\left(\frac{3}{4}+\sqrt{\mu s}+\mu s\right)}{(1+2\sqrt{\mu s})^2}\|v_k\|^2+2\mu\|y_{k-1}-x^\star\|^2. \quad (5.13)$$

Comparing the coefficients of the corresponding terms in (5.12) and (5.13) for $\mathcal{E}(k+1)$, we obtain that the iterative difference of the discrete Lyapunov function satisfies

$$\mathcal{E}(k+1)-\mathcal{E}(k)\leq -\sqrt{\mu s}\min\left\{1,\frac{1+\sqrt{\mu s}}{\frac{3}{4}+\sqrt{\mu s}+\mu s},\frac{1}{4}\right\}\mathcal{E}(k+1)-\frac{s(1-sL)}{2}\|G_s(y_k)\|^2.$$

We conclude here with the initial values $x_0\in\mathbb{R}^d$ and $v_0=0$. □

If we retrogress to the smooth case, the Lyapunov function (5.3) constructed by using x_k instead of y_k becomes more perfect than [Chen et al., 2022b, Theorem 4.2] in terms of the initial values. Taking a comparison between Theorem 4.1 and Theorem 5.1, we can find a little difference for the constant in the convergence rate. However, different from the smooth case, we cannot use $L\|x_0-x^\star\|^2$ to bound $\Phi(x_0)-\Phi(x^\star)+\mu\|x_0-x^\star\|^2$ obtained in (5.4) and (5.5) for the composite function, since the L-smooth inequality does not work anymore. To make the constant in the convergence rate consistent with Theorem 4.1, we need to start from $\mathcal{E}(1)$ in (5.3) as

$$\begin{aligned}\mathcal{E}(1) &= \Phi(x_1)-\Phi(x^\star)+\frac{\|v_1\|^2}{4(1+2\sqrt{\mu s})^2}+\frac{\|v_1+2\sqrt{\mu}(x_1-x^\star)\|^2}{4}\\ &\leq \Phi(x_1)-\Phi(x^\star)+\frac{\left(\frac{3}{4}+\sqrt{\mu s}+\mu s\right)}{(1+2\sqrt{\mu s})^2}\|v_1\|^2+2\mu\|x_0-x^\star\|^2, \quad (5.14)\end{aligned}$$

where the inequality follows from (5.13). Taking some basic calculations, we obtain $v_1=\sqrt{s}G_s(x_0)$ and put it into (5.14) as

$$\mathcal{E}(1)\leq \Phi(x_1)-\Phi(x^\star)+\frac{\left(\frac{3}{4}+\sqrt{\mu s}+\mu s\right)}{(1+2\sqrt{\mu s})^2}\cdot s\|G_s(x_0)\|^2+2\mu\|x_0-x^\star\|^2. \quad (5.15)$$

Similarly, putting x_1 generated by FISTA and the unique minimizer $x^\star$ into (3.5), we can see that Lemma 3.1 brings about the following inequality as

$$\Phi(x_1)-\Phi(x^\star)\leq \langle G_s(x_0),x_0-x^\star\rangle-\frac{s}{2}\|G_s(x_0)\|^2.$$

Furthermore, with perfect square and Cauchy-Schwarz inequality, we have the following two inequalities

$$\Phi(x_1) - \Phi(x^\star) \leq \frac{\|x_0 - x^\star\|^2}{2s} \qquad \text{and} \qquad \|G_s(x_0)\|^2 \leq \frac{4\|x_0 - x^\star\|^2}{s^2}$$

holds for any $0 < s \leq 1/L$. Hence, we conclude this section with the following corollary.

Corollary 5.2. *Let $\Phi = f + g$ be a composite function with $f \in \mathcal{S}^1_{\mu,L}(\mathbb{R}^d)$ and $g \in \mathcal{F}^0(\mathbb{R}^d)$. If the step size $0 < s \leq 1/L$, the iterative sequence $\{y_k\}_{k=0}^\infty$ generated by FISTA satisfies*

$$\Phi(x_k) - \Phi(x^\star) \leq \frac{11\|x_0 - x^\star\|^2}{2s\left(1 + \frac{\sqrt{\mu s}}{4}\right)^k}; \tag{5.16}$$

if the step size is set $s = 1/L$, we have

$$\Phi(x_k) - \Phi(x^\star) \leq \frac{11L\|x_0 - x^\star\|^2}{2\left(1 + \frac{1}{4}\sqrt{\frac{\mu}{L}}\right)^k}. \tag{5.17}$$

Furthermore, if $0 < s < 1/L$, the iterative sequence $\{y_k\}_{k=0}^\infty$ satisfies

$$\|G_s(y_k)\| \leq \frac{11\|x_0 - x^\star\|^2}{s^2(1 - sL)\left(1 + \frac{\sqrt{\mu s}}{4}\right)^k}. \tag{5.18}$$

6 Conclusion and discussion

In this paper, we improve the pivotal inequality for composite optimization found in [Li et al., 2022, Lemma 3.1], which becomes tighter with the convexity of the smooth part substituted by the μ-strongly convexity. Then, we apply the Lyapunov analysis to obtain the linear convergence for ISTA in both the objective value and the squared s-proximal subgradient norm. Meanwhile, we also use the Lyapunov analysis via the phase-space representation from the implicit-velocity scheme to derive the accelerated linear convergence for FISTA in both the objective value and the squared s-proximal subgradient norm. Looking back to the numerical experiment of FISTA in Figure 3, we can compute the constant μ to set the momentum coefficient. However, for the image deblurring problem in practice, it is so hard to compute the constant μ directly that we can set the momentum coefficient only empirically. Nevertheless, when we set the constant $\mu = 0.001$ in the numerical experiment of deblurring the image of an elephant, FISTA indeed converges faster than ISTA, which is shown in Figure 4. Therefore, how to provide an available constant μ in practice, e.g., for the blur matrix, looks very interesting.

The l_1-norm is widely used in the statistics, such as the Lasso model and its variants, as the regularizer to capture the sparse structure. An interesting direction is to investigate further the theory in statistics related to Lasso based on the new discoveries of the composite optimization theory. For example, the sorted l_1-penalized estimation (SLOPE) is proposed to capture adaptively unknown sparsity in the asymptotic minimax problem [Su and Candès, 2016], and the Lasso path involves a strong relation to false discoveries in [Su et al., 2017]. In addition, the differential inclusion used for sparse recovery [Osher et al., 2016] is also worth further consideration in the future since is strongly related to composite optimization.

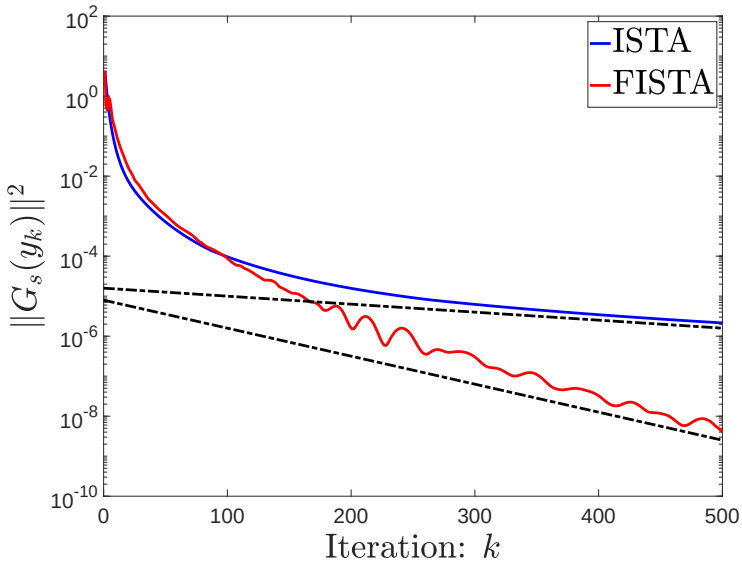

Figure 4: The convergence behavior of the squared s-proximal subgradient norm by implementing ISTA and FISTA to deblur the image of an elephant, previously shown in [Li et al., 2022, Figure 1 & Figure 2].

Acknowledgments

We would like to thank Shuo Chen for his helpful discussions.

References

H. Attouch, J. Peypouquet, and P. Redont. A dynamical approach to an inertial forward-backward algorithm for convex minimization. *SIAM Journal on Optimization*, 24(1):232–256, 2014.

H. Attouch, Z. Chbani, J. Fadili, and H. Riahi. First-order optimization algorithms via inertial systems with hessian driven damping. *Mathematical Programming*, pages 1–43, 2020.

A. Beck and M. Teboulle. A fast iterative shrinkage-thresholding algorithm for linear inverse problems. *SIAM Journal on Imaging Sciences*, 2(1):183–202, 2009.

S. Chen, B. Shi, and Y.-X. Yuan. Gradient norm minimization of nesterov acceleration: $o(1/k^3)$. *arXiv preprint arXiv:2209.08862*, 2022a.

S. Chen, B. Shi, and Y.-X. Yuan. Revisiting the high-resolution phenomenon via high-resolution differential equations. *arXiv preprint arXiv:2212.05700*, 2022b.

H. W. Engl, M. Hanke, and A. Neubauer. *Regularization of Inverse Problems*, volume 375. Springer Science & Business Media, 1996.

M. A. Figueiredo, R. D. Nowak, and S. J. Wright. Gradient projection for sparse reconstruction: Application to compressed sensing and other inverse problems. *IEEE Journal of Selected Topics in Signal Processing*, 1(4):586–597, 2007.

P. C. Hansen, J. G. Nagy, and D. P. O'leary. *Deblurring Images: Matrices, Spectra, and Filtering*. SIAM, 2006.

M. I. Jordan. Dynamical, symplectic and stochastic perspectives on gradient-based optimization. In *Proceedings of the International Congress of Mathematicians: Rio de Janeiro 2018*, pages 523–549. World Scientific, 2018.

B. Li, B. Shi, and Y.-X. Yuan. Proximal subgradient norm minimization of ISTA and FISTA. *arXiv preprint arXiv:2211.01610*, 2022.

Y. Nesterov. *Introductory Lectures on Convex Optimization: A Basic Course*, volume 87. Springer Science & Business Media, 1998.

Y. Nesterov. Recent advances in structural optimization. In *Proceedings of the International Congress of Mathematicians 2010 (ICM 2010) (In 4 Volumes) Vol. I: Plenary Lectures and Ceremonies Vols. II–IV: Invited Lectures*, pages 2964–2978. World Scientific, 2010.

Y. E. Nesterov. A method for solving the convex programming problem with convergence rate $O(1/k^2)$. *Dokl. Akad. Nauk SSSR*, 269:543–547, 1983.

S. Osher, F. Ruan, J. Xiong, Y. Yao, and W. Yin. Sparse recovery via differential inclusions. *Applied and Computational Harmonic Analysis*, 41(2):436–469, 2016.

B. T. Polyak. Some methods of speeding up the convergence of iteration methods. *USSR Computational Mathematics and Mathematical Physics*, 4(5):1–17, 1964.

R. T. Rockafellar. *Convex Analysis*, volume 18. Princeton University Press, 1970.

B. Shi, S. S. Du, W. Su, and M. I. Jordan. Acceleration via symplectic discretization of high-resolution differential equations. *Advances in Neural Information Processing Systems*, 32, 2019.

B. Shi, S. S. Du, M. I. Jordan, and W. J. Su. Understanding the acceleration phenomenon via high-resolution differential equations. *Mathematical Programming*, 195(1):79–148, 2022.

W. Su and E. Candès. SLOPE is adaptive to unknown sparsity and asymptotically minimax. *The Annals of Statistics*, 44(3):1038–1068, 2016.

W. Su, S. Boyd, and E. J. Candes. A differential equation for modeling Nesterov's accelerated gradient method: Theory and insights. *Journal of Machine Learning Research*, 17:1–43, 2016.

W. Su, M. Bogdan, and E. Candes. False discoveries occur early on the lasso path. *The Annals of Statistics*, pages 2133–2150, 2017.